Int. J. Heat Mass Transfer. Vol. 28, No. 8, pp. 1507–1515, 1985
Printed in Great Britain

0017-9310/85 $3.00 + 0.00

Calculation of the geometric-mean transmittance in a multi-dimensional absorbing and anisotropically-scattering medium

W. W. YUEN and W. DUNAWAY
Department of Mechanical and Environmental Engineering, University of California, Santa Barbara, CA 93106, U.S.A.

(*Received* 11 *October* 1984 *and in final form* 12 *February* 1985)

Abstract—Radiative heat transfer in an anisotropically-scattering medium is considered. Limiting expressions for the scattering contribution to the geometric-mean transmittance are developed. Using the kernel substitution technique, these expressions are evaluated analytically to provide closed form expressions for three selected two-dimensional geometries. These expressions allow conclusions to be drawn about the effect of anisotropic scattering in multi-dimensional systems.

1. INTRODUCTION

SCATTERING has been shown to play an important role in radiative heat transfer in many engineering systems [1]. An important parameter in practical calculations is the geometric-mean transmittance. The scattering contribution to this parameter has been calculated in a limiting fashion for a multi-dimensional medium which scatters isotropically [2]. However, most materials scatter anisotropically rather than isotropically. The anisotropic problem has been treated in several papers for systems with simple geometry [3, 4]. In addition, first-order approximations to the upper and lower limits of the scattering contribution to the geometric-mean transmittance have recently been generated for systems with more complex geometry [5].

The objective of this paper is to investigate how large the anisotropic effect can be in systems with multi-dimensional geometry. This paper will illustrate the effect of anisotropic scattering on radiative heat transfer by extending previous calculations [5] to higher orders.

Following a simple physical reasoning process [2], the present approach generalizes the previous first-order mathematical expressions [5] to give successively improved estimates of the scattering contribution to the geometric-mean transmittance in terms of upper and lower limits. The rate of convergence of each of these limits can be slow for selected cases. The two limits together, however, give a relatively narrow bound on the scattering contribution.

2. MATHEMATICAL DEVELOPMENT

2.1. *General formulation*

The equation for the transfer of energy by radiation between two arbitrary infinitesimal areas dA_0 and dA is

$$dQ_{d0-dA} = q_{o,0}\, dA_0\, dF_{d0-dA}(\tau_{d0-dA} + \tau^s_{d0-dA}) \quad (1)$$

where $q_{o,0}$ is the radiative heat flux leaving dA_0; dF_{d0-dA} is the shape factor between dA_0 and dA; τ_{d0-dA} is the geometric-mean transmittance between dA_0 and dA calculated only along the line of sight between dA_0 and dA; and τ^s_{d0-dA} is the scattering contribution to the geometric-mean transmittance due to scattering from elements away from the line of sight.

Expressions for τ_{d0-dA} are well known [6, 7]. An exact expression for τ^s_{d0-dA} is quite complicated. In the previous work [5], first-order approximations for the upper and lower limits of τ^s_{d0-dA} were generated for an anisotropically scattering medium by considering only radiation that leaves dA_0 and is scattered by a single volume element. Using the phase function

$$P(\cos \nu) = 1 + x_0 \cos \nu, \quad -1 \leqslant x_0 \leqslant 1 \quad (2)$$

where ν is the angle between the incoming and scattered radiation and x_0 is a forward–backward scattering parameter and utilizing a coordinate system as shown in Fig. 1, the first-order approximations for the upper and lower limits of τ^s_{d0-dA} were shown to be

$$dF_{d0-dA}[\tau^s_{d0-dA}]^1_u = \frac{\sigma}{\pi} \int\int\int \frac{z_1\, e^{-Er_1}}{r_1^3}\, dx_1\, dy_1\, dz_1 \quad (3)$$

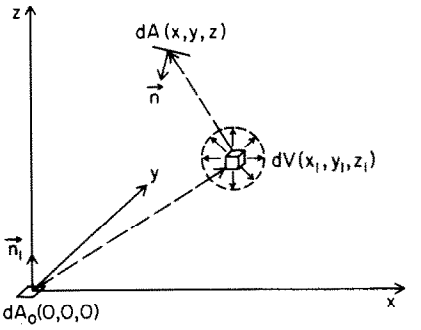

FIG. 1. Coordinate system and geometry for the calculation of the first-order approximation of the geometric-mean transmittance.

NOMENCLATURE

a	absorption coefficient
A	area
A_n	coefficient defined by equation (24)
B_n	coefficient defined by equation (24)
$C^n_{k,s}$	functions for recursive relations
$D^n_{k,s}$	functions for recursive relations
E	extinction coefficient
E_n	coefficient given by equation (38)
$E_n(X)$	function defined by equation (37)
F_n	coefficient given by equation (38)
$\mathrm{d}F$	shape factor between differential areas
F	shape factor
G	function defined by equations (10) and (11)
$M_{i,i-1}$	length defined by equation (19)
M_{nA}	length defined by equation (20)
$M^n_{k,s}$	function for recursive relations
$N^n_{k,s}$	function for recursive relations
P	phase function
Q	energy transfer
q_0	outgoing radiosity
$\mathbf{r}_{i,i-1}$	vector defined by equation (12)
$\mathbf{r}_{na}$	vector defined by equation (13)
R_1	expression given by equation (4a)
R_2	expression given by equation (4b)
$S_n(X)$	exponential integral function
x_0	scattering parameter for phase function
x	coordinate
y	coordinate
z	coordinate.

Greek symbols

θ	angle defined by equations (14) and (15)
τ	geometric transmittance factor
σ	scattering coefficient
ν	angle associated with phase function
β	function defined by equations (21) and (22)
ω	scattering albedo.

Subscripts

0	parameter associated with $\mathrm{d}A$
d0–dA	between areas $\mathrm{d}A_0$ and $\mathrm{d}A$
i	ith scattering element
l	lower limit
u	upper limit.

Superscripts

n	order of approximation
s	scattering contribution.

$$\mathrm{d}F_{\mathrm{d0-d}A}[\tau^{\mathrm{s}}_{\mathrm{d0-d}A}]^1_{\mathrm{l}} = \frac{\sigma}{4\pi^2}\,\mathrm{d}A(R_1 + x_0 R_2) \tag{4}$$

where

$$R_1 = \int\int\int \frac{z_1(\mathbf{n}\cdot\mathbf{r}_{1A})\,\mathrm{e}^{-E(r_1+r_{1A})}}{(r_1 r_{1A})^3}\,\mathrm{d}x_1\,\mathrm{d}y_1\,\mathrm{d}z_1 \tag{4a}$$

$$R_2 = -\int\int\int \frac{z_1(\mathbf{n}\cdot\mathbf{r}_{1A})(\mathbf{r}_1\cdot\mathbf{r}_{1A})\,\mathrm{e}^{-E(r_1+r_{1A})}}{(r_1 r_{1A})^4} \times \mathrm{d}x_1\,\mathrm{d}y_1\,\mathrm{d}z_1 \tag{4b}$$

with

$$E = a + \sigma \tag{5}$$

$$\mathbf{r}_1 = x_1\hat{\mathbf{i}} + y_1\hat{\mathbf{j}} + z_1\hat{\mathbf{k}} \tag{6}$$

and

$$\mathbf{r}_{1A} = (x_1 - x)\hat{\mathbf{i}} + (y_1 - y)\hat{\mathbf{j}} + (z_1 - z)\hat{\mathbf{k}}. \tag{7}$$

In these expressions, $\mathrm{d}A_0$ is assumed to be a diffuse surface; a and σ are the absorption and scattering coefficients of the medium; $\hat{\mathbf{i}}$, $\hat{\mathbf{j}}$, and $\hat{\mathbf{k}}$ are unit vectors in the x, y and z directions; $\mathbf{n}$ is the unit normal to the surface $\mathrm{d}A$; and r_1 and r_{1A} are the magnitudes of the vectors $\mathbf{r}_1$ and $\mathbf{r}_{1A}$.

To improve the accuracy of the estimates of the upper and lower limits these results may be generalized to include scattering from multiple volume elements. Using the same physical reasoning utilized previously for isotropic scattering [2], it can be shown that the expressions for the nth approximation can be written in terms of the expressions for the $(n-1)$th approximation as

$$\mathrm{d}F_{\mathrm{d0-d}A}[\tau^{\mathrm{s}}_{\mathrm{d0-d}A}]^n_{\mathrm{u}} = \mathrm{d}F_{\mathrm{d0-d}A}[\tau^{\mathrm{s}}_{\mathrm{d0-d}A}]^{n-1}_{\mathrm{l}} + G^n_{\mathrm{u}} \tag{8}$$

$$\mathrm{d}F_{\mathrm{d0-d}A}[\tau^{\mathrm{s}}_{\mathrm{d0-d}A}]^n_{\mathrm{l}} = \mathrm{d}F_{\mathrm{d0-d}A}[\tau^{\mathrm{s}}_{\mathrm{d0-d}A}]^{n-1}_{\mathrm{l}} + G^n_{\mathrm{l}} \tag{9}$$

where

$$G^n_{\mathrm{u}} = \left(\frac{\sigma}{\pi}\right)\left(\frac{\sigma}{4\pi}\right)^{n-1}\int\cdots\int\frac{z_1\,\mathrm{e}^{-Er_1}}{r_1^3} \times \left(\prod_{i=1}^{n}\frac{(1+x_0\cos\theta_{i,i-1})}{r^2_{i,i-1}}\,\mathrm{e}^{-Er_{i,i-1}} \times \mathrm{d}x_i\,\mathrm{d}y_i\,\mathrm{d}z_i\right)\mathrm{d}x_1\,\mathrm{d}y_1\,\mathrm{d}z_1 \tag{10}$$

$$G^n_{\mathrm{l}} = \left(\frac{\sigma}{4\pi}\right)^n\frac{\mathrm{d}A}{\pi}\int\cdots\int\frac{z_1(\mathbf{n}\cdot\mathbf{r}_{nA})\,\mathrm{e}^{-E(r_1+r_{nA})}}{(r_1 r_{nA})^3} \times (1+x_0\cos\theta_{nA})\left(\prod_{i=2}^{n}\frac{(1+x_0\cos\theta_{i,i-1})}{r^2_{i,i-1}} \times \mathrm{e}^{-Er_{i,i-1}}\,\mathrm{d}x_i\,\mathrm{d}y_i\,\mathrm{d}z_i\right)\mathrm{d}x_1\,\mathrm{d}y_1\,\mathrm{d}z_1 \tag{11}$$

and

$$\mathbf{r}_{i,i-1} = (x_i - x_{i-1})\hat{\mathbf{i}} + (y_i - y_{i-1})\hat{\mathbf{j}} + (z_i - z_{i-1})\hat{\mathbf{k}} \quad (12)$$

$$\mathbf{r}_{nA} = (x_n - x)\hat{\mathbf{i}} + (y_n - y)\hat{\mathbf{j}} + (z_n - z)\hat{\mathbf{k}} \quad (13)$$

$$\cos\theta_{i,i-1} = \frac{\mathbf{r}_{i-1,i-2} \cdot \mathbf{r}_{i,i-1}}{r_{i-1,i-2}\, r_{i,i-1}} \quad (14)$$

$$\cos\theta_{nA} = \frac{\mathbf{r}_{nA} \cdot \mathbf{r}_{n,n-1}}{r_{nA}\, r_{n,n-1}}. \quad (15)$$

In these expressions (x_i, y_i, z_i) is the coordinate of the ith scattering volume.

It is to be expected from physical considerations that in the limit as n approaches infinity the upper limit will decrease and the lower limit will increase monotonically toward the exact value. The rate of convergence, however, can be quite slow, particularly for systems with a small scattering albedo. It is therefore much more efficient to consider both limits simultaneously, placing a bound on the exact value at an arbitrary value of n.

2.2. *Two-dimensional systems*

If the areas dA and dA_0 are considered to be infinite strips, the problem becomes two-dimensional. If dA has width dS and a unit normal vector given by

$$\mathbf{n} = l\hat{\mathbf{i}} + n\hat{\mathbf{k}} \quad (16)$$

then equations (8) and (9) still hold and equations (10) and (11) can be integrated over

$$-\infty < y_i < \infty \quad i = 1, n$$

to yield

$$G_u^n = \left(\frac{\sigma^n}{4^{n-1}}\right) \int \cdots \int \frac{z_1 S_2(EM_1)}{M_1^2} \left(\prod_{i=2}^{n} \frac{S_1(EM_{i,i-1})}{M_{i,i-1}} \times (1 + x_0 \beta_{i,i-1})\, dx_i\, dx_i \right) dx_1\, dz_1 \quad (17)$$

and

$$G_l^n = \left(\frac{\sigma}{4}\right)^n dS \int \cdots \int z_1 [(x_n - x)l + (z_n - z)n] \times \frac{S_2(EM_1) S_2(EM_{nA})}{M_1^2 M_{nA}^2} (1 + x_0 \beta_{nA}) \times \left(\prod_{i=2}^{n} \frac{S_1(EM_{i,i-1})}{M_{i,i-1}} (1 + x_0 \beta_{i,i-1}) \times dx_i\, dz_i \right) dx_1\, dz_1 \quad (18)$$

where

$$M_i = [(x_i - x_{i-1})^2 + (z_i - z_{i-1})^2]^{1/2} \quad (19)$$

$$M_{nA} = [(x_n - x)^2 + (z_n - z)^2]^{1/2} \quad (20)$$

$$\beta_{i,i-1} = \frac{\mathbf{M}_i \cdot \mathbf{M}_{i-1}}{M_i M_{i-1}} S_1(EM_i) S_1(EM_{i-1}) \quad (21)$$

and

$$\beta_{nA} = \frac{\mathbf{M}_n \cdot \mathbf{M}_{nA}}{M_n M_{nA}} S_1(EM_n) S_1(EM_{nA}). \quad (22)$$

In these expressions $S_n(x)$ is the exponential integral function given by

$$S_n(x) = \frac{\sigma^n}{\pi} \int_{-\infty}^{\infty} \frac{e^{-(x^2+y^2)^{1/2}}}{[x^2+y^2]^{(n+1)/2}}\, dy \quad (23)$$

which has been studied extensively [2, 8]. To carry out many of the required integrations, it is convenient to introduce the following kernel substitution:

$$S_n(x) = A_n e^{-B_n x}. \quad (24)$$

The constants A_n and B_n have been determined in previous considerations [2, 8].

Equations (8), (9), (17) and (18), together with equations (3) and (4), are a complete set which can be used to calculate the upper and lower limits of τ^s_{d0-dA} to any desired degree of accuracy.

3. APPLICATION

As in previous work [2, 5], the equations will be applied to three selected geometries. The approach will be used to generate recursive relations which give results at an arbitrary n in terms of the results for $(n-1)$. The geometries considered are the same as those in the above references.

3.1. *Case 1*

Consider A to be an infinite horizontal plate facing downward toward dA_0 at an optical thickness Ez, as shown in Fig. 2(a). For this case the limits of integration are

$$-\infty < x_i < \infty \qquad i = 1, n$$

$$-\infty < x < \infty$$

$$-\infty < z_i < z \qquad i = 2, n$$

$$0 < z_i < z.$$

It can be shown that G_u^n and G_l^n become

$$G_u^n = 4\left(\frac{\omega}{4}\right)^n M_{0,0}^n \quad (25)$$

and

$$G_l^n = \left(\frac{\omega}{4}\right)^n N_{2,0}^n \quad (26)$$

where ω is the scattering albedo and

$$M_{k,s}^n = \mathrm{I}_{k,s}^n + x_0 \mathrm{II}_{k,s}^n \quad (27)$$

$$N_{k,s}^n = C_{k,s}^n + x_0 D_{k,s}^n \quad (28)$$

$$C_{k,s}^n = \mathrm{III}_{k,s}^n + x_0 \mathrm{IV}_{k,s}^n \quad (29)$$

$$D_{k,s}^n = \mathrm{V}_{k,s}^n + x_0 \mathrm{VI}_{k,s}^n. \quad (30)$$

Recursive relations for the functions I–VI, are listed in the appendix, along with the appropriate expressions for starting the iterative process. These expressions,

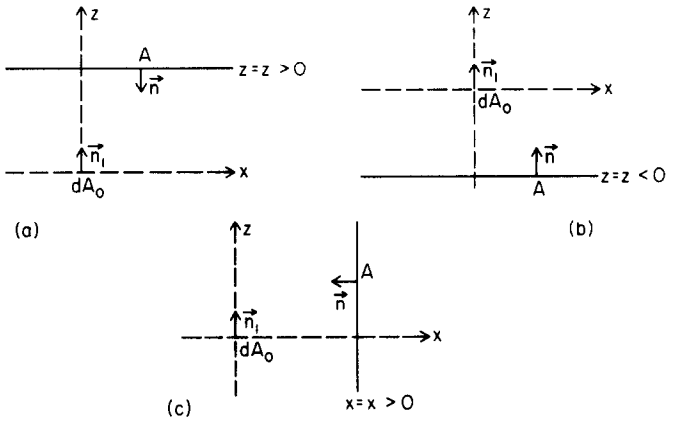

FIG. 2. Geometries of the three specific cases for dA_0 and A considered in the present work.

along with equations (8) and (9), can be used to calculate the scattering contribution to the geometric-mean transmittance for this particular geometry.

3.2. *Case 2*

In this case, A is an infinite plate facing upward at a distance $-z$ below dA_0 as shown in Fig. 2(b). The limits of integration are

$$-\infty < x_i < \infty \qquad i = 1, n$$
$$-\infty < x < \infty$$
$$-z < z_i < \infty \qquad i = 2, n$$
$$0 < z_1 < \infty.$$

For this case, the functions G_u^n and G_l^n are

$$G_u^n = 4\left(\frac{\omega}{4}\right)^n M^n \tag{31}$$

$$G_l^n = \left(\frac{\omega}{4}\right)^n N_{2,0}^n \tag{32}$$

where

$$M^n = I^n + x_0 \mathrm{II}^n \tag{33}$$

$$N_{k,s}^n = C_{k,s}^n + x_0 D_{k,s}^n \tag{34}$$

$$C_{k,s}^n = \mathrm{III}_{k,s}^n + x_0 \mathrm{IV}_{k,s}^n \tag{35}$$

$$D_{k,s}^n = \mathrm{V}_{k,s}^n + x_0 \mathrm{VI}_{k,s}^n. \tag{36}$$

Recursive relations and starting expressions for this case are given in the appendix.

3.3. *Case 3*

In this case, A is an infinite plate placed vertically at a distance x from dA_0 as shown in Fig. 2(c). The new limits of integration are

$$-\infty < x_i < x \qquad i = 1, n$$
$$-\infty < z < \infty$$
$$-\infty < z_i < \infty \qquad i = 2, n$$
$$0 < z_i < \infty.$$

After integration it is found that equations (25)–(30) hold for this case, with x replacing z. The recursive relations are the same as for case 1, and therefore it is only necessary to determine the starting relations. Two additional kernel substitutions are needed for $E_1(x)$ and $E_2(x)$, which are the familiar exponential functions [7]. These expressions are

$$E_1(x) = 2e^{-2x} \tag{37}$$

$$E_2(x) = e^{-2x}. \tag{38}$$

Utilizing equations (37) and (38), limiting values of the geometric mean transmittance are evaluated using expressions derived in the appendix.

4. RESULTS AND DISCUSSION

The rate of convergence for this method is illustrated in Figs. 3 and 4 for Case 1 with optical thickness equal to 1. It is similar for other cases and optical thicknesses. The scattering albedo ω plays a large part in determining the rate of convergence, with cases with small albedo converging quickly. This is because G_u^n and G_l^n are both proportional to ω^n. In some instances oscillatory behavior was noticed for large values of n. This is attributed to error introduced by the kernel substitution.

Numerical results for the three cases are presented in Tables 1, 2 and 3. In some cases the value given is the best estimate, with the computation being truncated at the n beyond which numerical oscillation began. For purposes of comparison, values of the geometric-mean transmittance calculated without the scattering contribution are included in the tables.

To illustrate the relative importance of the various scattering parameters (ω and x_0) and the optical thickness (Ez or Ex) on the heat transfer, the average of the best estimate of the upper and lower limits of $F_{dO-A}\tau_{dO-A}^s$ for the three cases are plotted in Figs. 5–7. Some important conclusions concerning the general effect of anisotropic scattering can be readily generated.

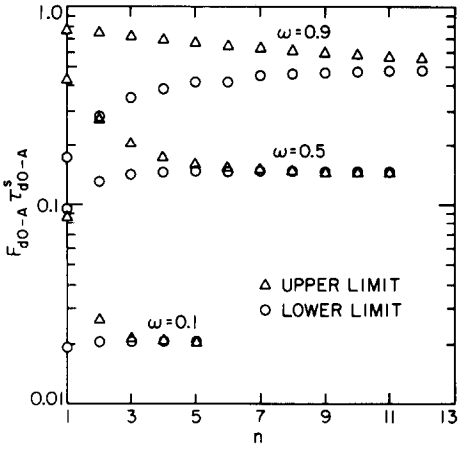

FIG. 3. The convergence behavior for Case 1 with $Ez = 1.0$, $x_0 = 1.0$.

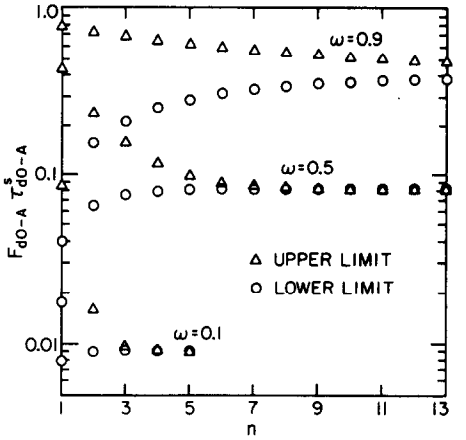

FIG. 4. Convergence behavior for Case 1 with $Ez = 1.0$, $x_0 = -1.0$.

Table 1. The lower and upper limits of $F_{dO-A}\tau^s_{dO-A}$ calculated for Case 1

		$x_0 = 0$		$x_0 = 1$		$x_0 = -1$		
Ez	ω	Lower	Upper	Lower	Upper	Lower	Upper	$F_{dO-A}\tau_{dO-A}$
	0.1	0.8479×10^{-2}	0.8479×10^{-2}	0.1055×10^{-1}	0.1056×10^{-1}	0.6642×10^{-2}	0.6648×10^{-2}	
0.1	0.5	0.5062×10^{-2}	0.5062×10^{-1}	0.5882×10^{-1}	0.5885×10^{-1}	0.4317×10^{-1}	0.4320×10^{-1}	0.8326
	0.9	0.1285	0.1302	0.1350	0.1402	0.1234	0.1315	
	0.1	0.1950×10^{-1}	0.1950×10^{-1}	0.2545×10^{-1}	0.2547×10^{-1}	0.1371×10^{-1}	0.1371×10^{-1}	
0.5	0.5	0.1304	0.1304	0.1595	0.1596	0.1049	0.1050	0.4432
	0.9	0.4035	0.4122	0.4336	0.4687	0.3776	0.4186	
	0.1	0.1477×10^{-1}	0.1472×10^{-1}	0.2059×10^{-1}	0.2059×10^{-1}	0.9082×10^{-2}	0.9087×10^{-2}	
1	0.5	0.1125	0.1126	0.1481	0.1426	0.8272×10^{-1}	0.8277×10^{-1}	0.2194
	0.9	0.4518	0.4696	0.4912	0.5737	0.3808	0.4806	
	0.1	0.4155×10^{-2}	0.4156×10^{-2}	0.6931×10^{-2}	0.6931×10^{-2}	0.1555×10^{-2}	0.1555×10^{-2}	
2	0.5	0.4071×10^{-1}	0.4075×10^{-1}	0.6407×10^{-1}	0.6411×10^{-1}	0.2302×10^{-1}	0.2307×10^{-1}	0.0602
	0.9	0.2890	0.3239	0.3351	0.4924	0.1974	0.3768	

Table 2. The lower and upper limits of $F_{dO-A}\tau^s_{dO-A}$ for Case 2

		$x_0 = 0$		$x_0 = 1$		$x_0 = -1$		
Ez	ω	Lower	Upper	Lower	Upper	Lower	Upper	$F_{dO-A}\tau_{dO-A}$
	0.1	0.2648×10^{-1}	0.2648×10^{-1}	0.1815×10^{-1}	0.1815×10^{-1}	0.3481×10^{-1}	0.3481×10^{-1}	
0	0.5	0.1779	0.1781	0.1397	0.1398	0.2200	0.2201	0
	0.9	0.5782	0.5955	0.5401	0.6518	0.2207	0.8009	
	0.1	0.2192×10^{-1}	0.2193×10^{-1}	0.1488×10^{-1}	0.1489×10^{-1}	0.2899×10^{-1}	0.2900×10^{-1}	
0.1	0.5	0.1552	0.1553	0.1265	0.1266	0.1882	0.1882	0
	0.9	0.5490	0.5682	0.5185	0.6638	0.6411	0.7491	
	0.1	0.1025×10^{-1}	0.1026×10^{-1}	0.6637×10^{-2}	0.6644×10^{-2}	0.1395×10^{-2}	0.1392×10^{-2}	
0.5	0.5	0.8803×10^{-1}	0.8809×10^{-1}	0.8027×10^{-1}	0.8111×10^{-1}	0.9934×10^{-1}	0.9937×10^{-1}	
	0.9	0.4330	0.4585	0.4644	0.6315	0.4681	0.5837	
	0.1	0.3928×10^{-2}	0.3929×10^{-2}	0.2333×10^{-2}	0.2334×10^{-2}	0.5611×10^{-2}	0.5612×10^{-2}	
1	0.5	0.4182×10^{-1}	0.4186×10^{-1}	0.4156×10^{-1}	0.4176×10^{-1}	0.4385×10^{-1}	0.4389×10^{-1}	0
	0.9	0.3059	0.3407	0.2941	0.5622	0.2912	0.4317	
	0.1	0.5647×10^{-3}	0.5648×10^{-3}	0.2400×10^{-3}	0.2401×10^{-3}	0.9282×10^{-3}	0.9283×10^{-3}	
2	0.5	0.8761×10^{-2}	0.8767×10^{-2}	0.9824×10^{-2}	0.9920×10^{-2}	0.8234×10^{-2}	0.8252×10^{-2}	0
	0.9	0.1424	0.1911	0.1014	0.4535	0.1571	0.2799	

Table 3. The lower and upper limits of $F_{d0-A}\tau^s_{d0-A}$ calculated for Case 3

		$x_0 = 0$		$x_0 = 1$		$x_0 = -1$		
Ez	ω	Lower	Upper	Lower	Upper	Lower	Upper	$F_{d0-A}\tau_{d0-A}$
0	0.1	0.1478×10^{-1}	0.1479×10^{-1}	0.1147×10^{-1}	0.1148×10^{-1}	0.1800×10^{-1}	0.1800×10^{-1}	
	0.5	0.9759×10^{-1}	0.9766×10^{-1}	0.9765×10^{-1}	0.7973×10^{-1}	0.1128	0.1128	0.5000
	0.9	0.2963	0.3333	0.2758	0.3231	0.3157	0.3586	
0.1	0.1	0.1749×10^{-1}	0.1749×10^{-1}	0.1563×10^{-1}	0.1563×10^{-1}	0.1928×10^{-1}	0.1928×10^{-1}	
	0.5	0.1166	0.1167	0.1047	0.1048	0.1261	0.1262	0.3480
	0.9	0.3600	0.4059	0.3403	0.4000	0.3875	0.4286	
0.5	0.1	0.1660×10^{-1}	0.1661×10^{-1}	0.1746×10^{-1}	0.1747×10^{-1}	0.1573×10^{-1}	0.1573×10^{-1}	
	0.5	0.1216	0.1217	0.1249	0.1250	0.1176	0.1176	0.1409
	0.9	0.4408	0.5231	0.4536	0.5342	0.4590	0.5299	
1	0.1	0.9447×10^{-2}	0.9454×10^{-2}	0.1072×10^{-1}	0.1073×10^{-1}	0.8202×10^{-2}	0.8209×10^{-2}	
	0.5	0.7974×10^{-1}	0.7980×10^{-1}	0.8920×10^{-1}	0.8925×10^{-1}	0.7094×10^{-1}	0.7100×10^{-1}	0.5822×10^{-1}
	0.9	0.3771	0.4858	0.3978	0.5261	0.4029	0.4741	
2	0.1	0.1948×10^{-2}	0.1949×10^{-2}	0.2490×10^{-2}	0.2491×10^{-2}	0.1437×10^{-2}	0.1438×10^{-2}	
	0.5	0.2204×10^{-1}	0.2206×10^{-1}	0.2893×10^{-1}	0.2903×10^{-1}	0.1639×10^{-1}	0.1639×10^{-1}	0.1203×10^{-1}
	0.9	0.1920	0.3368	0.2208	0.3952	0.1470	0.3473	

As demonstrated in previous studies for isotropic scattering [2], the scattering contribution to the geometric-mean transmittance is extremely important for media with large scattering albedo. In all three cases (except for the optically thin limit in case one for which the geometric-mean transmittance is one), scattering contributes over 50% to the total geometric-mean transmittance when $\omega = 0.9$.

In general, the effect of the anisotropic factor x_0 is most significant in systems with large optical thickness and small but finite scattering albedo. In media with large scattering albedo, photons leaving the area dA_0 are scattered many times before they are absorbed by the area A. Since each photon can experience multiple scattering involving different scattering angles, the detailed angular dependence of the scattering function is 'averaged out' and the effect of x_0 is thus less significant.

For cases in which the effect of x_0 is significant, however, the specific effect of anisotropic scattering appears to be quite complex and depends strongly on the geometry of the considered system. In case 1, for example, $F_{d0-A}\tau^s_{d0-A}$ for a medium with $x_0 = 1.0$ (strongly forward scattering) is always higher than those with $x_0 = 0$ (isotropic scattering) and $x_0 = -1$ (strongly backward scattering). In cases 2 and 3, on the other hand, the heat transfer in a strongly forward scattering medium can be higher (case 2, $\omega = 0.9$, $Ez = 1.0$, 2.0 and Case 3, $\omega = 0.1$, 0.5, $Ex = 1.0$, 2.0) or lower (case 2, $\omega = 0.1$; $\omega = 0.5, 0.9$, $Ez = 0.1$ and Case 3, $\omega = 0.1$, 0.5, $Ex = 0.5$) than the corresponding isotropic scattering and strongly-backward scattering

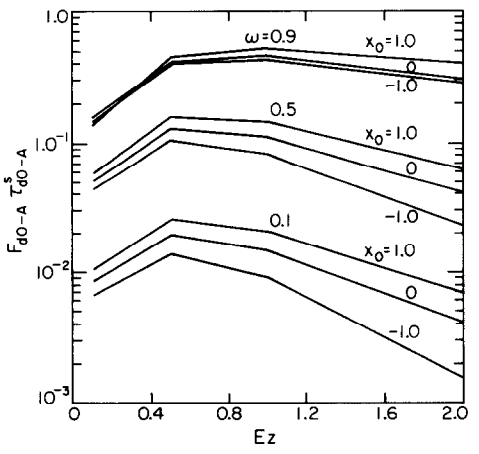

FIG. 5. Effects of ω and x_0 on $F_{d0-A}\tau^s_{d0-A}$ at different optical thickness for Case 1.

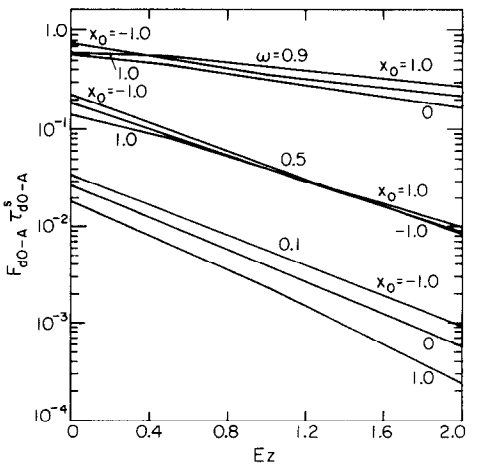

FIG. 6. Effects of ω and x_0 on $F_{d0-A}\tau^s_{d0-A}$ at different optical thickness for Case 2.

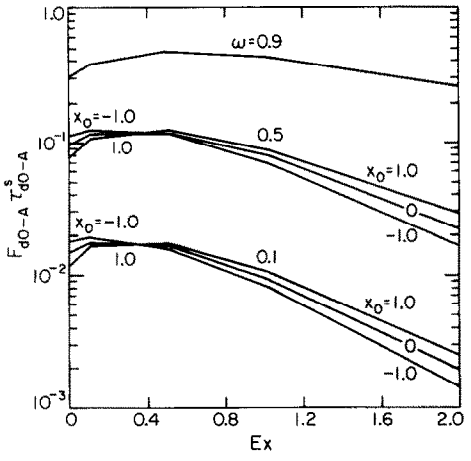

FIG. 7. Effects of ω and x_0 on $F_{dO-A}\tau^s_{dO-A}$ at different optical thickness for Case 3.

cases. In case 2 with $\omega = 0.9$, it is interesting to note that both anisotropic cases ($x_0 = 1.0$ and $x_0 = -1.0$) yield higher heat transfer than the corresponding isotropic case when the optical thickness is large ($Ez = 1.0, 2.0$).

Physically, the difference in the effect of x_0 on the heat transfer for the three cases is due primarily to the difference in geometry of the three scattering media. In case 1, the area A is in the 'forward' direction relative to dA_0. An increase in the forward scattering thus naturally leads to an increase in heat transfer. In case 2, a photon leaving dA_0 must undergo both forward and backward scatterings before it is absorbed by the area A. The overall effect of anisotropic scattering on the net heat transfer thus becomes a sensitive function of the scattering albedo and optical thickness. This same argument also explains the complicated effect of x_0 observed for case 3.

In recent years, many investigators [4, 9, 10] have attempted to develop 'scaling' relations so that heat transfer in anisotropic scattering media can be expressed in terms of 'equivalent' isotropic scattering results. Most of the mathematics developed for such 'scaling' relations, however, were based on analyses of a one-dimensional parallel slab. The present work shows that the applicability of such 'scaling' relations to scattering media with non-parallel-slab geometries can be highly uncertain. Indeed, the sensitive dependence on geometry as illustrated in this work suggests that the development of 'scaling' relations for general multi-dimensional anisotropic scattering media might be an extremely difficult task.

Acknowledgement—This work is based partially upon work supported by the National Science Foundation Grant Number MEA 80-24824.

REFERENCES

1. J. DeRis, Fire radiation, a review. *The 17th Symposium (International) on Combustion*, pp. 1003–1006. Combustion Institute (1979).
2. W. W. Yuen, A limiting approach for the evaluation of geometric-mean transmittance in a multi-dimensional absorbing and isotropically scattering medium, *Trans. Am. Soc. mech. Engrs, J. Heat Transfer* **106**, 441–447 (1984).
3. L. S. Dolin, Propagation of a narrow beam of light in a medium with strongly anisotropic scattering, *Sov. Radiophys.* **9**, 40–47 (1966).
4. H. Lee and R. O. Buckius, Scaling anisotropic scattering in radiation heat transfer for a planar medium, *Trans. Am. Soc. mech. Engrs, J. Heat Transfer* **104**, 68–75 (1982).
5. W. W. Yuen, Evaluation of geometric-mean transmittance in a multi-dimensional absorbing and anisotropically scattering medium, ASME Paper 83-HT-45.
6. H. C. Hottel and A. F. Sarofim, *Radiative Transfer*, Chap. 7. McGraw-Hill, New York (1967).
7. R. Siegel and J. R. Howell, *Thermal Radiation Heat Transfer*, Chap. 17. McGraw-Hill, New York (1972).
8. W. W. Yuen and L. W. Wong, Numerical computation of an important integral function in two-dimensional radiative transfer, *J. quant. Spectrosc. Rad. Transfer* **29**, 145–149 (1983).
9. B. H. T. McKellar and M. A. Box, The scaling group of radiative transfer equation. *J. atmos. Sci.* **38**, 1063 (1981).
10. E. Inönü, Scaling and time reversal for the linear monoenergetic Brefzmann equation. In *Topics in Mathematical Physics* (edited by H. Odabasi and O. Akyuz), p. 113. Colorado Associated University Press (1977).

APPENDIX

Recursive relations for Case 1

$$I^n_{k,s} = \left[\sum_{r=0}^{s} \frac{(-1)^r s!\,(Ez)^{s-r}}{(s-r)!\,(-B_{k+1}B_k)^{r+1}}\right] C^{n-1}_{k+1,0} + \pi A_k A_{k+1} \sum_{r=0}^{s} \frac{(-1)^r s!}{(s-r)!}\left[\frac{(-1)^k - 1}{(-B_k B_{k+1})^{r+1}}\right] M^{n-1}_{0,s-r} \quad \text{(A1)}$$

$$II^n_{k,s} = \left[\sum_{r=0}^{s} \frac{(-1)^r s!\,(Ez)^{s-r}}{(s-r)!\,(-B_{k+1}B_{k+2})}\right] D^{n-1}_{k+1,0} + \pi A_{k+1} A_{k+2} \sum_{r=0}^{s} \frac{(-1)s!}{(s-r)!}\left[\frac{(-1)^{k+1} - 1}{(-B_{k+1}B_{k+2})^{r+1}}\right] M^{n-1}_{1,s-r} \quad \text{(A2)}$$

$$III^n_{k,s} = \pi A_1 A_0 \sum_{r=0}^{s} \frac{(-1)^r s!\, C^{n-1}_{k,s-r}}{(s-r)!} \times \left[\frac{1}{(B_k B_{k-1} + B_1 B_0)^{r+1}} \frac{1}{(B_k B_{k-1} - B_1 B_0)^{r+1}}\right] + \pi A_k A_{k-1} C^{n-1}_{1,0} \sum_{r=0}^{s} \frac{(-1)^r s!\,(Ez)^{s-r}}{(s-r)!\,(B_k B_{k-1} - B_1 B_0)^{r+1}}, \quad k \neq 1 \quad \text{(A3)}$$

$$III^n_{1,s} = \pi A_1 A_0 \sum_{r=0}^{s} \frac{(-1)^r s!\, C^{n-1}_{1,s-r}}{(s-r)!\,(2B_1 B_0)^{r+1}} + \frac{\pi A_k A_{k-1}}{s+1}(Ez)^{s+1} C^{n-1}_{1,0} - \frac{\pi A_k A_{k-1}}{s+1} C^{n-1}_{1,s+1} \quad \text{(A4)}$$

$$IV^n_{k,s} = -\pi A_2 A_1 \sum_{r=0}^{s} \frac{(-1)^r s!\, D^{n-1}_{k-1,s-r}}{(s-r)!} \times \left[\frac{1}{(B_k B_{k-1} + B_1 B_2)^{r+1}} + \frac{1}{(B_k B_{k-1} - B_1 B_2)^{r+1}}\right] + \pi A_k A_{k-1} D^{n-1}_{1,0} \sum_{r=0}^{s} \frac{(-1)^r s!\,(Ez)^{s-r}}{(s-r)!\,(B_k B_{k-1} - B_1 B_2)^{r+1}}, \quad k \neq 2 \quad \text{(A5)}$$

$$\mathrm{IV}^n_{2,s} = -\pi A_2 A_1 \sum_{r=0}^{s} \frac{(-1)^r s!\, D^{n-1}_{1,s-r}}{(s-r)!\,(2B_1B_2)^{r+1}} + \frac{\pi A_1 A_2}{s+1}\left[(Ez)^{s+1} D^{n-1}_{1,0} - D^{n-1}_{1,s+1}\right] \quad \text{(A6)}$$

$$\mathrm{V}^n_{k,s} = -\pi A_2 A_1 \sum_{r=0}^{s} \frac{(-1)^r s!\, C^{n-1}_{k+1,s-r}}{(s-r)!} \times \left[\frac{1}{(B_{k+1}B_k + B_1B_2)^{r+1}} + \frac{1}{(B_{k+1}B_k - B_1B_2)^{r+1}}\right] + \pi A_{k+1}A_k C^{n-1}_{2,0} \sum_{r=0}^{s} \frac{(-1)^r s!\,(Ez)^{s-r}}{(s-r)!\,(B_{k+1}B_k - B_1B_2)^{r+1}}, \quad k \neq 1 \quad \text{(A7)}$$

$$\mathrm{V}^n_{1,s} = -\pi A_2 A_1 \sum_{r=0}^{s} \frac{(-1)^r s!\, C^{n-1}_{2,s-r}}{(s-r)!\,(2B_1B_2)^{r+1}} + \frac{\pi A_2 A_1}{s+1}\left[(Ez)^{s+1} C^{n-1}_{2,0} - C^{n-1}_{2,s+1}\right] \quad \text{(A8)}$$

$$\mathrm{VI}^n_{k,s} = \pi A_3 A_2 \sum_{r=0}^{s} \frac{(-1)^r s!\, D^{n-1}_{k,s-r}}{(s-r)!} \times \left[\frac{1}{(B_{k+1}B_k + B_2B_3)^{r+1}} - \frac{1}{(B_{k+1}B_k - B_2B_3)^{r+1}}\right] + \pi A_{k+1} + A_k D^{n-1}_{2,0} \sum_{r=0}^{s} \frac{(-1)^r s!\,(Ez)^{s-r}}{(s-r)!\,(B_{k+1}B_k - B_2B_3)^{r+1}}, \quad k \neq 2 \quad \text{(A9)}$$

$$\mathrm{V}^n_{2,s} = \pi A_3 A_2 \sum_{r=0}^{s} \frac{(-1)^r s!\, D^{n-1}_{2,s-r}}{(s-r)!(2B_2B_3)^{r+1}} + \frac{\pi A_3 A_2}{s+1}\left[(Ez)^{s+1} D^{n-1}_{2,0} - D^{n-1}_{2,s+1}\right]. \quad \text{(A10)}$$

Starting equations for Case 1

$$C^1_{k,s} = \pi^2 A_k A_{k-1} A_2 A_1 \left[\mathrm{e}^{-B_1B_2Ez} \times \sum_{r=0}^{s} \left(\frac{(-1)^r s!\,(Ez)^{s-r}}{(s-r)!\,(B_kB_{k-1} - B_2B_1)^{r+1}}\right) - \frac{(-1)^s s!\, \mathrm{e}^{-B_kB_{k-1}Ez}}{(B_{k-1}B_k - B_2B_1)^{s+1}}\right], \quad k \neq 2 \quad \text{(A11)}$$

$$C^1_{2,s} = \frac{(\pi A_2 A_1)^2\, \mathrm{e}^{-B_2B_1Ez}(Ez)^{s+1}}{s+1} \quad \text{(A12)}$$

$$D^1_{k,s} = \pi^2 A_{k+1} A_k A_3 A_2 \left[\mathrm{e}^{-B_2B_3Ez} \times \sum_{r=0}^{s} \left(\frac{(-1)^r s!\,(Ez)^{s-r}}{(s-r)!\,(B_kB_{k+1} - B_3B_2)^{r+1}}\right) - \frac{(-1)^s s!\, \mathrm{e}^{-B_kB_{k+1}Ez}}{(B_kB_{k+1} - B_3B_2)^{s+1}}\right], \quad k \neq 2 \quad \text{(A13)}$$

$$D^1_{2,s} = \frac{(\pi A_3 A_2)\, \mathrm{e}^{-B_2B_3Ez}(Ez)^{s+1}}{s+1} \quad \text{(A14)}$$

$$M^1_{k,s} = \pi A_{k+2} A_{k+1} \left[\mathrm{e}^{-B_{k+2}B_{k+1}Ez} \times \sum_{r=0}^{s} \left(\frac{(-1)^r s!\,(Ez)^{s-r}}{(s-r)!\,(-B_{k+2}B_{k+1})^{r+1}}\right) - \frac{(-1)^s s!}{(-B_{k+2}B_{k+1})^{s+1}}\right]. \quad \text{(A15)}$$

Recursive relations for Case 2

$$\mathrm{I}^n = \frac{2\pi A_1 A_0}{B_1B_0} G^{n-1}_u - \frac{1}{B_1B_0} C^{n-1}_{1,0} \quad \text{(A16)}$$

$$\mathrm{II}^n = \frac{1}{B_2B_1} D^{n-1}_{1,0} \quad \text{(A17)}$$

$$\mathrm{III}^n_{k,s} = \pi A_1 A_0 \sum_{r=0}^{s} \frac{s!}{(s-r)!}\left[\frac{(-1)^r}{(B_1B_0 - B_kB_{k-1})^{r+1}} + \frac{1}{(B_1B_0 + B_kB_{k-1})^{r+1}}\right] C^{n-1}_{k,s-r} - \pi A_k A_{k-1}(-1)^s \times \left[\sum_{r=0}^{s} \frac{s!\,(Ez)^{s-r}}{(s-r)!\,(B_1B_0 - B_kB_{k-1})^{r+1}}\right] C^{n-1}_{1,0}, \quad k \neq 1 \quad \text{(A18)}$$

$$\mathrm{III}^n_{1,s} = \frac{\pi A_1 A_0}{s+1}\left[C^{n-1}_{1,s+1} + (-1)^s (Ez)^{s+1} C^{n-1}_{1,0}\right] + \pi A_1 A_0 \sum_{r=0}^{s} \frac{s!\, C^{n-1}_{1,s-r}}{(s-r)!\,(2B_1B_0)^{r+1}} \quad \text{(A19)}$$

$$\mathrm{IV}^n_{k,s} = \pi A_2 A_1 \sum_{r=0}^{s} \frac{s!}{(s-r)!}\left[\frac{1}{(B_1B_2 + B_kB_{k-1})^{r+1}} - \frac{(-1)^r}{(B_2B_1 - B_kB_{k-1})^{r+1}}\right] D^{n-1}_{k-1,s-r} + \pi A_k A_{k-1} D^{n-1}_{1,0}(-1)^s \times \sum_{r=0}^{s} \frac{s!\,(Ez)^{s-r}}{(s-r)!\,(B_2B_1 - B_kB_{k-1})^{r+1}}, \quad k \neq 2 \quad \text{(A20)}$$

$$\mathrm{IV}^n_{1,s} = \frac{\pi A_1 A_2}{s+1}\left[(-Ez)^{s+1} D^{n-1}_{1,0} - D^{n-1}_{1,s+1}\right] + \pi A_2 A_1 \sum_{r=0}^{s} \frac{s!\, D^{n-1}_{1,s-r}}{(s-r)!\,(2B_1B_2)^{r+1}} \quad \text{(A21)}$$

$$\mathrm{V}^n_{k,s} = \pi A_2 A_1 \sum_{r=0}^{s} \frac{s!}{(s-r)!}\left[\frac{(-1)^r}{(B_1B_2 - B_{k+1}B_k)^{r+1}} - \frac{1}{(B_1B_2 + B_{k+1}B_k)^{r+1}}\right] C^{n-1}_{k+1,s-r} - \pi A_{k+1} A_k C^{n-1}_{2,0}(-1)^s \times \sum_{r=0}^{s} \frac{s!\,(Ez)^{s-r}}{(s-r)!\,(B_2B_1 - B_{k+1}B_k)^{r+1}}, \quad k \neq 1 \quad \text{(A22)}$$

$$\mathrm{V}^n_{1,s} = \frac{\pi A_2 A_1}{s+1}\left[C^{n-1}_{2,s+1} - (-Ez)^{s+1} C^{n-1}_{2,0}\right] - \pi A_2 A_1 \sum_{r=0}^{s} \frac{s!\, C^{n-1}_{2,s-r}}{(s-r)!\,(2B_2B_1)^{r+1}} \quad \text{(A23)}$$

$$\mathrm{VI}^n_{k,s} = -\pi A_3 A_2 \sum_{r=0}^{s} \frac{s!}{(s-r)!}\left[\frac{(-1)^r}{(B_3B_2 - B_{k+1}B_k)^{r+1}} + \frac{1}{(B_3B_2 + B_{k+1}B_k)^{r+1}}\right] D^{n-1}_{k,s-r} + \pi A_{k+1} A_k D^{n-1}_{2,0}(-1)^s \times \sum_{r=0}^{s} \frac{s!\,(Ez)^{s-r}}{(s-r)!\,(B_3B_2 - B_{k+1}B_k)^{r+1}}, \quad k \neq 2 \quad \text{(A24)}$$

$$\mathrm{VI}^n_{2,s} = -\frac{\pi A_3 A_2}{s+1}\left[D^{n-1}_{2,s+1} + (-1)^s (Ez)^{s+1} D^{n-1}_{2,0}\right] + \pi A_3 A_2 \sum_{r=0}^{s} \frac{s!\, D^{n-1}_{2,s-r}}{(s-r)!\,(2B_2B_3)^{r+1}}. \quad \text{(A25)}$$

Starting equations for Case 2

$$G_u^1 = \frac{\pi A_2 A_1}{B_2 B_1} \tag{A26}$$

$$C_{k,s}^1 = \frac{\pi^2 A_1 A_2 A_{k-1} A_k s!}{(B_k B_{k-1} + B_2 B_1)^{s+1}} e^{-B_k B_{k-1} Ez} \tag{A27}$$

$$D_{k,s}^1 = \frac{-\pi^2 A_2 A_3 A_k A_{k+1}}{(B_{k+1} B_k + B_3 B_2)^{s+1}} e^{-B_{k+1} B_k Ez}. \tag{A28}$$

Recursive relations for Case 3

The recursive relations for Case 3 are given by equations (A1)–(A10), inclusive.

Starting equations for Case 3

$$C_{k,s}^1 = \pi A_k A_{k-1} A_2 E_1 e^{-B_k B_{k-1} Ex} \times \left[\frac{(-1)^s}{(B_k B_{k-1} + F_1 B_2)^{s+1}} - \frac{(-1)^s s!}{(B_k B_{k-1} - B_2 F_1)^{s+1}} \right] + e^{-B_2 F_1 Ex} \sum_{r=0}^{s} \frac{(-1)^r s! (Ex)^{s-r}}{(s-r)! (B_k B_{k-1} - B_2 F_1)^{r+1}}. \tag{A29}$$

If $B_k B_{k-1} = B_2 F_1$

$$C_{k,s}^1 = \pi A_k A_{k-1} A_2 E_1 e^{-B_k B_{k-1} Ex} \times \left[\frac{(-1)^s s!}{(B_k B_{k-1} + F_1 B_2)^{s+1}} + \frac{(Ex)^{s+1}}{s+1} \right] \tag{A30}$$

$$D_{k,s}^1 = \pi A_{k+1} A_k A_3 E_2 e^{-B_{k+1} B_k Ex} \times \left[\frac{-(-1)^s s!}{(B_k B_{k+1} + B_3 F_2)^{s+1}} - \frac{(-1)^s s!}{(B_k B_{k+1} - B_3 F_2)^{s+1}} \right] + e^{-F_2 B_3 Ex} \sum_{r=0}^{s} \frac{(-1)^r s! (Ex)^{s-r}}{(s-r)! (B_k B_{k+1} - B_3 F_2)^{r+1}}. \tag{A31}$$

If $B_{k+1} B_k = B_3 F_2$

$$D_{k,s}^1 = \pi A_{k+1} A_k A_3 E_2 e^{-B_{k+1} B_k Ex} \times \left[\frac{-(-1)^s s!}{(B_{k+1} B_k + F_2 B_3)^{s+1}} + \frac{(Ex)^{s+1}}{s+1} \right] \tag{A32}$$

$$M_{0,0}^1 = \frac{A_2 E_1}{F_1 B_2} (2 - e^{-F_1 B_2 Ex}). \tag{A33}$$

CALCUL DE LA TRANSMITTANCE MOYENNE GEOMETRIQUE DANS UN MILIEU ABSORBANT MULTIDIMENSIONNEL ET DIFFUSANT ANISOTROPIQUEMENT

Résumé—On considère le rayonnement thermique dans un milieu diffusant anisotropiquement. Des expressions limitantes sont développées pour la contribution de la diffusion à la transmittance moyenne géométrique. En utilisant la technique de substitution de noyau, ces expressions sont évaluées analytiquement pour fournir des expressions analytiques pour des géométries bidimensionnelles particulières. Ces expressions fournissent des conclusions utiles sur l'effet de la diffusion anisotrope dans des systèmes multidimensionnels.

DIE BERECHNUNG DES GEOMETRISCHEN MITTELWERTS DER DURCHLÄSSIGKEIT IN EINEM MULTIDIMENSIONALEN ABSORBIERENDEN UND ANISOTROP STREUENDEN MEDIUM

Zusammenfassung—Es wird die Wärmeübertragung durch Strahlung in einem anisotrop streuenden Medium untersucht. Es werden einschränkende Ausdrücke für den Beitrag der Streuung zum geometrischen Mittelwert der Durchlässigkeit entwickelt. Mit Hilfe des Kernel-Substitutionsverfahrens werden diese Ausdrücke analytisch ausgewertet, um Beziehungen in geschlossener Form für drei ausgewählte zweidimensionale Geometrien zu erhalten. Diese Beziehungen ermöglichen Schlußfolgerungen über den Einfluß anisotroper Streuung in multidimensionalen Systemen.

РАСЧЕТ В ГЕОМЕТРО-ОПТИЧЕСКОМ ПРИБЛИЖЕНИИ КОЭФФИЦИЕНТА ПРОПУСКАНИЯ В МНОГОМЕРНОЙ ПОГЛОЩАЮЩЕЙ И АНИЗОТРОПНО-РАССЕИВАЮЩЕЙ СРЕДЕ

Аннотация—Рассматривается радиационный теплоперенос в анизотропно-рассеивающей среде в геометро-оптическом приближении. Получены предельные выражения для оценки вклада рассеяния в коэффициент пропускания. Подстановкой ядра эти выражения преобразуются аналитически к замкнутой форме для трех выбранных двумерных геометрий. Полученные выражения позволяют сделать выводы об эффекте анизотропного рассеяния в многомерных системах.